

Article

Synthesis, Crystal Structure, and Luminescent Properties of a New Holmium(III) Coordination Polymer Involving 2,5-Dihydroxy-1,4-terephthalic Acid Dianion as Ligand

Jiaqi Li ^{1,2}, Linan Dun ³, Fanming Zeng ^{1,2,*}, Chun Li ^{1,2} and Zhongmin Su ^{1,2,*}

¹ School of Materials Science and Engineering, Changchun University of Science and Technology, Changchun 130022, China; chuanbl@jlu.edu.cn (J.L.); lichun@cust.edu.cn (C.L.)

² Jilin Provincial Science and Technology Innovation Center of Optical Materials and Chemistry, Changchun 130022, China

³ School of Materials Science and Engineering, Northeastern University, Shenyang 110006, China; 2110202@stu.neu.edu.cn

* Correspondence: zengfm@cust.edu.cn (F.Z.); zmsu@nenu.edu.cn (Z.S.)

Abstract: A novel coordination polymer $\{[\text{Ho}_2(\text{DHTA})_3(\text{H}_2\text{O})_5]\cdot\text{H}_2\text{O}\}_n$ (**1**) was synthesized by hydrothermal synthesis (DHTA = 2,5-dihydroxy-1,4-terephthalic acid anion). The crystallographic data show that complex **1** crystallizes in a triclinic system with space group $P\bar{1}$, with $a = 9.6617(17)$ Å, $b = 11.902(2)$ Å, $c = 13.284(2)$ Å, $\alpha = 100.617(3)^\circ$, $\beta = 92.765(2)^\circ$, $\gamma = 106.715(2)^\circ$, $V = 1429.6(4)$ Å³, $Z = 2$, $\text{C}_{24}\text{H}_{24}\text{O}_{24}\text{Ho}_2$, and $M_r = 1026.290$. Complex **1** contains two eight-coordinated metal centers Ho(III). The TGA results show that the weight loss can be ascribed to the removal of the organic component from 400 to 650 °C. At the temperature above 650 °C, the residue is Holmium(III) oxide (Ho_2O_3). The luminescent results reveal that the complex has potential application as a new green luminescence material.

Keywords: holmium(III); luminescence property; coordination polymer; crystal structure; 2,5-dihydroxyl-1,4-terephthalic acid



Citation: Li, J.; Dun, L.; Zeng, F.; Li, C.; Su, Z. Synthesis, Crystal Structure, and Luminescent Properties of a New Holmium(III) Coordination Polymer Involving 2,5-Dihydroxy-1,4-terephthalic Acid Dianion as Ligand. *Crystals* **2021**, *11*, 1294. <https://doi.org/10.3390/cryst11111294>

Academic Editors: Ana M. Garcia-Deibe and Jesús Sanmartín-Matalobos

Received: 21 September 2021
Accepted: 21 October 2021
Published: 26 October 2021

Publisher's Note: MDPI stays neutral with regard to jurisdictional claims in published maps and institutional affiliations.



Copyright: © 2021 by the authors. Licensee MDPI, Basel, Switzerland. This article is an open access article distributed under the terms and conditions of the Creative Commons Attribution (CC BY) license (<https://creativecommons.org/licenses/by/4.0/>).

1. Introduction

Metal-organic frameworks (MOFs) are organic-inorganic hybrid materials which are composed of inorganic nodes connected by organic ligands through the self-assembly process [1]. In recent years, MOFs have received a considerable amount of attention due to their diverse properties: luminescence, catalysis, magnetism, and gas adsorption, etc. [2,3]. In particular, MOFs have shown their applications in the luminescence area over the past decades; many strategies have been proposed to enhance the luminescence properties of the MOFs and have obtained some advanced material to detect heavy-metal ions and organic pollutants [4,5]. For example, Zhao et al. have used a solvothermal synthesized $\text{Cu}_3(\text{BTC})_2$ (HKUST-1) to adsorb Ce^{3+} from water. These results demonstrated a significantly intensive adsorption capacity and a rapid removal rate [6]. Yang et al. reported a robust luminescent zirconium-based MOF, PCN-128Y, which can serve as an excellent platform for both detection and removal of antibiotic tetracycline, it also exhibits favorable adsorption capability toward tetracycline in water [7]. In addition, rare earth metals, as functional metal centers, are attracting more and more attention due to their fantastic coordination properties and special chemical characteristics. Rare earth metals are fundamental to many industrial applications, which can be utilized as positive charged metal ions in MOFs, and they have shown immense potential in luminescence material due to their enhanced luminescence. One example of this is a 3D holmium(III) coordination framework based on the pyridine 2,6-dicarboxylate and oxalate ligands by Feng et al. [8]. Preliminary studies reveal this complex, with weak ferromagnetic couplings within the two adjacent magnetic centers bridged through oxalato group, displays characteristic

metal-centered fluorescence in solid state. In 2011, Czaja et al. reported the luminescence properties of rare-earth ions of natural fluorite; they proposed the most effective excitation mechanism for holmium ion emission [9]. It is demonstrated that $\lambda_{\text{exc}} = 415 \text{ nm}$ evidently enhances the green luminescence of Ho^{3+} ions, that is, the $^5\text{S}_2 \rightarrow ^5\text{I}_8$ transition. In addition, terbium and holmium co-doped yttrium phosphate as non-contact optical temperature sensors was successfully obtained by Fang and co-workers [10]. Thus far, coordination polymers of various structures have been obtained from metal ions, and carboxylic acid ligands through coordination bonds or intermolecular interactions, revealing potential applications in the field of functional materials [11]. The selection of appropriate organic ligand is also of significance to promote the luminescence properties of the MOFs [12–17]. Rare earth ions have high affinity for hard donor atoms and organic ligands containing oxygen or oxygen–nitrogen heteroatom, especially multicarboxylate [18]. In the past several years, carboxylic acid ligands, such as 2,5-dihydroxyl-1,4-terephthalic acid (DHTA), are of particular interest as linkers for luminescent MOFs synthesis. DHTA possess advantages over other organic ligands such as 1,10-phenanthroline in terms of multiple coordination sites, strong coordination ability, and high variety of coordination modes [19]. Though there are some reports about the carboxylic acid ligands coordinated with rare earth metals, the holmium(III) coordination frameworks are rarely reported. Thus, the combination of Ho(III) with DHTA may obtain new complexes with novel structures or particular properties. In this work, we present a new type of coordination polymer, $\{[\text{Ho}_2(\text{DHTA})_3(\text{H}_2\text{O})_5] \cdot \text{H}_2\text{O}\}_n$ (DHTA = 2,5-dihydroxyl-1,4-terephthalate), which is composed of Ho(III) and DHTA, in which the latter acts as both bidentate and tridentate bridging ligand. **1** was synthesized under hydrothermal conditions. The structure of **1** was confirmed by elemental analyses, IR spectrum, single-crystal X-ray diffraction analyses, and powder X-ray diffraction (PXRD). In addition, the TGA and luminescence property analysis revealed that **1** has high thermal stability and remarkable luminescence property. This work provides a new method to synthesize materials with excellent luminescent properties.

2. Experimental

2.1. Materials and Method

DHTA was synthesized according to reference [20,21]; the solvents were purified by distillation before use, and other reagents were used directly without further purification. $\text{Ho}(\text{NO}_3)_3 \cdot 6\text{H}_2\text{O}$ was obtained from Aladdin chemical reagent company (Energy Chemical Co., Ltd., Shanghai, China).

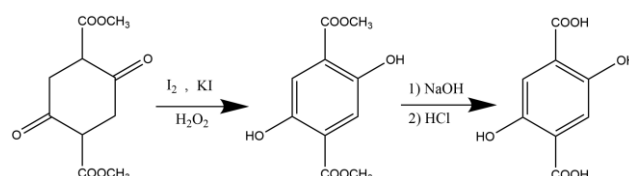
2.2. Characterization

Single-crystal X-ray data were obtained on a Bruker Smart Apex II CCD (Bruker AXS GmbH, Karlsruhe, Germany) based diffractometer equipped with graphite monochromatized $\text{Mo-K}\alpha$ radiation ($\lambda = 0.71073 \text{ nm}$) at 296 K. The C, H, N, and O elemental analyses were performed on a Perkin-Elmer 2400 elemental analyzer (PerkinElmer, Inc., Waltham, MA, USA). The luminescence properties have been studied using a Hitachi F-4600 spectrophotometer (Hitachi High-Tech Science Corporation, Tokyo, Japan) in the solid state at room temperature. In order to ensure the same conditions of fluorescence characterization of complex **1** and DHTA, we took the same amount of their samples and then ground them in a mortar for five minutes, respectively. The slit widths of excitation and emission were 2 nm. 3D excitation scans of the luminescence of **1** has been recorded $400 \text{ nm} \leq \lambda_{\text{ex}} \leq 700 \text{ nm}$. The wavelength was scanned at 20 nm/s; a solid sample of **1** was locked between two glass slides and then tested. The IR spectrum was recorded with a Shimadzu IR-408 spectrophotometer (Shimadzu Corporation, Kyoto, Japan) using the KBr pellet in the range of $4000\text{--}400 \text{ cm}^{-1}$. The thermal stability experiment was conducted on a TG SDT2960 thermal analyzer (TA Instruments, DE, USA) at a heating rate of $10 \text{ }^\circ\text{C}/\text{min}$ under nitrogen from room temperature to $800 \text{ }^\circ\text{C}$. PXRD was tested on a Rigaku RINT Ultima III diffractometer (Rigaku Industrial Corp., Tokyo, Japan) with $\text{Cu-K}\alpha$ radiation

($\lambda = 1.5418 \text{ \AA}$) by depositing powder on glass substrate, from $2\theta = 1.5^\circ$ up to 60° with 0.02° increment.

2.3. Synthesis of DHTA

The preparation of the DHTA is depicted in Scheme 1. For a typical process, 22 g (0.11 mol) of dimethyl 1,4-cyclohexanedione-2,5-dicarboxylate was dissolved in glacial acetic acid (120 mL) in a four-neck flask and stirred for an hour to obtain a homogeneous solution. Subsequently, the solution was heated to 120°C under reflux. After the addition of I_2 (0.3 g, 1.18 mmol) and potassium iodide (0.3 g, 1.8 mmol), 6 mL (57 mM) of hydrogen peroxide was added to the system dropwise. After refluxing, 50 mL of water was added into the solution and the temperature of the system was maintained 100°C for 2 h. The resulting product (yellow powder) was filtered and washed with distilled water three times and finally dried at 75°C for 12 h to obtain dimethyl 2,5-dihydroxyterephthalate. Next, 20 g (0.1 mol) of the dimethyl 2,5-dihydroxyterephthalate was mixed with water (100 mL) by stirring in a three-neck bottle, resulting in a yellow thick liquid. Subsequently, 8 g of sodium hydroxide was added into the above system. The solution was heated to 100°C under nitrogen purge and maintained for 2 h. Then, 57 mM hydrochloric acid was added to the solution dropwise until the pH of the solution was adjusted to 4.5. The resulting product was filtered, washed with distilled water 3 times, and the DHTA was obtained after vacuum drying at 80°C for 24 h (yield: 14.4 g, 80.16%). Anal. Calcd. for $\text{C}_8\text{H}_6\text{O}_6$ (%): C, 48.50; H, 3.05; O, 48.45. Found (%): C, 48.38; H, 3.09; O, 48.53. The standard uncertainties were calculated to be 0.06, 0.02, and 0.03 for C, H, and O, respectively. IR (KBr): 3076, 1647, 1459, 1429, 1359, 1186, 897, 850, and 755 cm^{-1} . $^1\text{H NMR}$ (400 MHz, DMSO): δ 10.887 (q, 2H), 7.290 (q, 2H), and 3.708 (q, 2H).



Scheme 1. Synthesis route of the DHTA.

2.4. Synthesis of $\{[\text{Ho}_2(\text{DHTA})_3(\text{H}_2\text{O})_5] \cdot \text{H}_2\text{O}\}_n$ (**1**)

The complex $\{[\text{Ho}_2(\text{DHTA})_3(\text{H}_2\text{O})_5] \cdot \text{H}_2\text{O}\}_n$ (**1**) was prepared by a hydrothermal method: $\text{Ho}(\text{NO}_3)_3 \cdot 6\text{H}_2\text{O}$ (0.1 mmol, 45.9 mg) and DHTA (0.15 mmol, 29.7 mg) were firstly dissolved in 12 mL distilled water and stirred for 0.5 h to obtain a homogeneous solution. Then, 5 mL of NaOH solution (0.25 M) was added to the solution and stirred for another 0.5 h at room temperature. The resultant solution was transferred into a 25 mL Teflon-lined stainless-steel autoclave. After hydrothermal treatment at 150°C for 3 days, the reaction mixture was cooled to room temperature and the resultant product was filtered by distilled water 3 times. The prepared **1** was primrose yellow block crystals. Yield: 30.0 mg (65.4% based on $\text{Ho}(\text{III})$). Anal. Calcd for $\text{C}_{24}\text{H}_{24}\text{Ho}_2\text{O}_{24}$: C, 28.14%; H, 2.41%, and O, 37.26%; Found: C, 28.08%; H, 2.36%; and O, 37.42%.

2.5. X-Ray Crystallography

Single-crystal diffraction data were collected at room temperature on an XRD-6100 lab diffractometer using a microfocus Mo $\text{K}\alpha$ emission rays ($\lambda = 0.71073 \text{ \AA}$). One primrose yellow single crystal with dimensions of $0.150 \text{ mm} \times 0.118 \text{ mm} \times 0.077 \text{ mm}$ was selected and mounted on a goniometer head using paraffin oil. A total of 6362 reflections were collected in the range of $1.569^\circ \leq \theta \leq 26.04^\circ$ using the ω - 2θ scan mode, of which 5682 were unique with $R_{\text{int}} = 0.0232$. The program CrysAlisPro was used to control the data collection and for the subsequent data reduction [22]. The crystal structure was solved using the direct methods program SHELX [23] and refined using SHELXL in Olex2 [24]. All non-hydrogen atoms were refined anisotropically. The hydrogen atoms were generated

geometrically and treated by a mixture of independent and constrained refinement. The crystal data and refinement details of the complex are summarized in Table 1. CCDC 1995993 contains the supplementary crystallographic data for this paper. These data can be obtained free of charge from The Cambridge Crystallographic Data Centre via www.ccdc.cam.ac.uk/data_request/cif (Accessed on 20 October 2021).

Table 1. Crystal Data and Structure Refinement for complex **1**.

Complex	1
Empirical formula	C ₂₄ H ₂₄ O ₂₄ Ho ₂
Formula weight	1026.29
Crystal system	<i>Triclinic</i>
Space group	<i>P</i> $\bar{1}$
Unit cell dimensions	a = 9.6617(17) Å, α = 100.617(3)° b = 11.902(2) Å, β = 92.765(2)° c = 13.284(2) Å, γ = 106.715(2)°
Volume	1429.6(4) Å ³
Z	2
Density (calculated)	2.384 g/cm ³
F(000)	982
Theta range for data collection	1.569 to 26.04°
Independent reflections	6362 [R _{int} = 0.0232]
Goodness-of-fit on F ²	1.078
Final R indices [I > 2 sigma(I)]	R ₁ = 0.0321, wR ₂ = 0.0819
R indices (all data)	R ₁ = 0.0360, wR ₂ = 0.0835

3. Results and Discussions

3.1. Structure Description

The coordination environment of Ho(III) in **1** is depicted in Figure 1 and the corresponding crystallographic data are summarized in Table 1. Independent parts of the unit cell of **1** are composed of two independent Ho(III) centers, seven DHTA ligands, and six water molecules. One of the DHTA acts as tridentate bridging ligand, connecting the two Ho(III) through one hydroxyl oxygen atom and two carbonyl oxygen atoms; the other DHTA ligands around the Ho(III) are all bidentate ligands. The two Ho(III) are located in two different environments, and their coordination modes are different, but both are eight-coordinated. To be specific, the Ho1 is bound to eight oxygen atoms, five of which are from four different DHTA ligands and the other three are from three aqua ligands, forming a slightly distorted square antiprism (Figure 2). Similarly, the Ho2 is bound to eight oxygen atoms, among which six are from four different DHTA ligands as well, and the remaining two oxygen atoms come from aqua ligands. The coordination modes form a slightly distorted square antiprism. Interestingly, the DHTA ligands possess four different coordination manners (A, B, C, and D), as shown in Scheme 2: the DHTA which contains O1 atom is connected with four Ho(III) atoms (manner A), while DHTA containing O10, O16, or O21, are connected the two Ho atoms (manner B, C, or D, respectively). In coordination mode C, the DHTA bridged the adjacent Ho(III) ions and extended the crystal in different directions to form a three-dimensional supramolecular network structure (Figure 3). The selected bond lengths and bond angles are listed in Table S1.

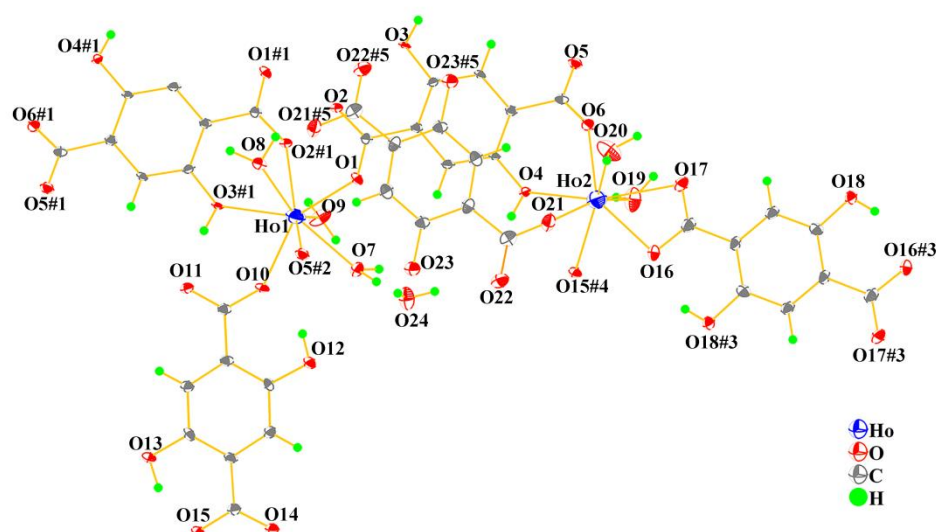


Figure 1. Coordination environment of the coordination complex 1. (Symmetry codes for #1: 1-x, 2-y, 2-z; #2: x-1, y, z; #3: 2-x, -y, 1-z; #4: -x, 1-y, 1-z; and #5: 1-x, 1-y, 2-z.)

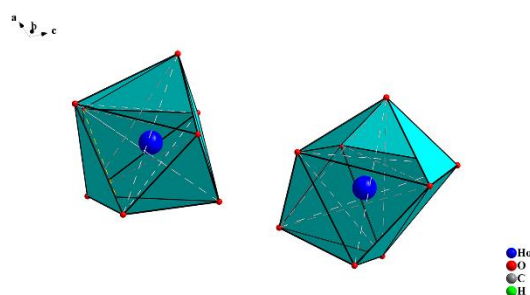
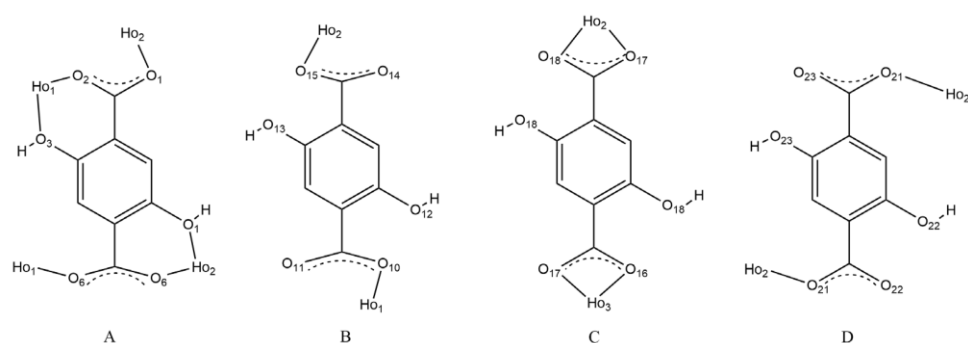


Figure 2. The coordination polyhedra of the holmium atoms.



Scheme 2. Four connection manners of DHTA unit (the oxygen atom labels are consistent with the name given in cif).

From Table S2, the distance between Ho-O_{carboxyl} is 2.238 to 2.500 Å, and the distances between Ho-O_{water} vary from 2.316 to 2.594 Å, which is in agreement with the bond lengths observed in other Ho(III) complexes [25]. In the network structure, there are two types of hydrogen bond, namely, C-H...O and O-H...O (presented in Figure 4 and Table S2). In addition, two types of intermolecular π ... π and C-H... π interactions exist in the arrangement; as shown in Table S3, the hydrogen bonds and π ... π interactions enriched the architecture of 1. The distances between the center of gravity of the π rings (Cg...Cg distance) ranges from 3.730 to 3.742 Å, and the distances between C atom and Cg of the π rings (C...Cg distance) range from 3.371 and 3.850 Å. Generally, the co-existence of π ... π , [26–28] C-H... π interactions and hydrogen bonds makes complex 1 become more

stable, which contributes to the forming of a more stable three-dimensional network structure, as shown in Figure 3.

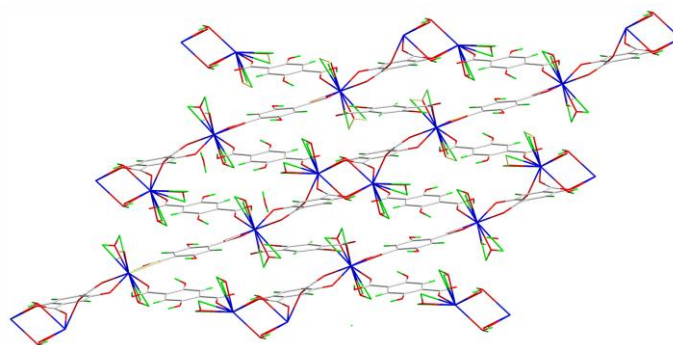


Figure 3. The 3D supramolecular meshy structure of complex 1.

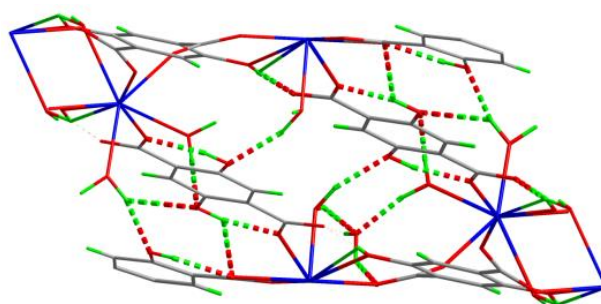


Figure 4. Hydrogen bonds (green dotted line).

3.2. IR Analysis

The IR spectra of the complex **1** and DHTA are shown in Figure 5. From the infrared spectrum of complex **1**, the main characteristic peaks of **1** are 3392, 1587, 1503, 1441, 1371, 1204, 912, 870, and 786 cm^{-1} , and the main characteristic peaks of DHTA are 3076, 1647, 1459, 1429, 1359, 1186, 897, 850, and 755 cm^{-1} , respectively. There are wide and strong absorption bands in the range of 3500–3200 cm^{-1} ; it should be ascribed by the characteristic stretching vibration of hydroxyl groups from water molecules, the association of hydrogen bonds may result in the broadening of the peaks. The band of the COO group from DHTA ligand at 1647 cm^{-1} completely vanished in the spectrum of the complex **1**, indicating no free carboxyl group in complex **1**. The peak at 1587 cm^{-1} was assigned to asymmetric vibrations of the COO group, and the peaks at 1371 cm^{-1} was assigned to symmetric vibrations of the COO group. The shift shows that carboxyl groups participate in the coordination [29,30]. The characteristic peaks of substituted aromatic rings are mainly at 912, 870, and 786 cm^{-1} . IR spectrum of the complex was consistent with the structure analysis from the X-ray diffraction.

3.3. Thermogravimetric Analysis

The stability of **1** was investigated by thermogravimetric (TGA) analysis experiment. In the temperature range of 40–1000 $^{\circ}\text{C}$, the complex **1** experienced two significant weight loss processes. As shown in Figure 6, from 40 $^{\circ}\text{C}$ to 95 $^{\circ}\text{C}$, it shows a weight loss of 2.00%, which is ascribed to the removal of one free water molecule (calculated 1.80%). Between 152 and 200 $^{\circ}\text{C}$, it shows a weight loss of 8.90%, which is ascribed to the removal of five coordinating water (calculated 8.80%). After 250 $^{\circ}\text{C}$, it is due to the decomposition of molecules of the organic component. Surprisingly, we found that the weight loss did not stop, even at 1000 $^{\circ}\text{C}$; this phenomenon may be due to the strong thermal stability of the complex, resulting in slow weight loss.

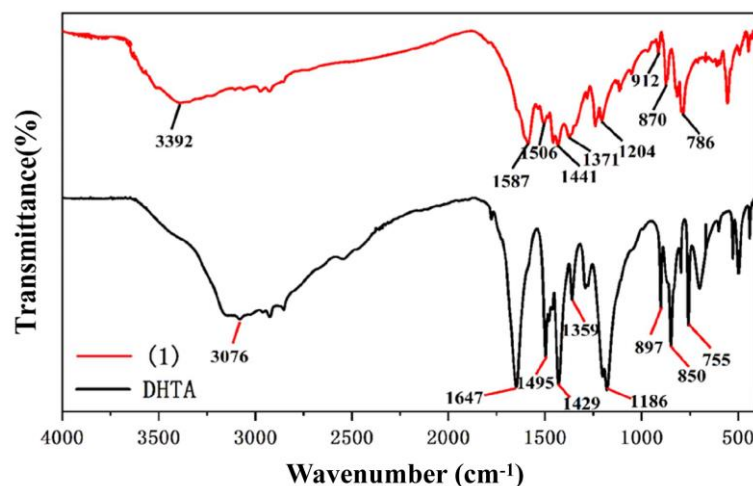


Figure 5. IR spectra of 1 and DHTA.

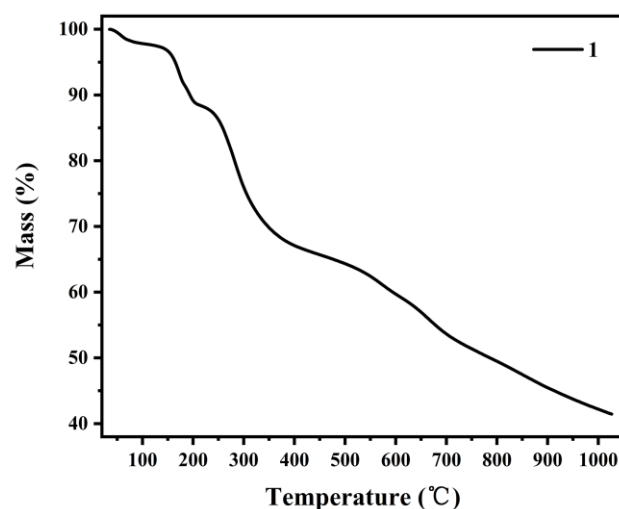


Figure 6. TG curve of complex 1.

3.4. PXRD Analysis

PXRD analysis of complex 1 was performed at room temperature. The PXRD pattern of complex 1 as-synthesized are basically consistent with the simulated samples (Figure 7), though slightly different from the simulated pattern at the low angled peaks due to minor impurities.

3.5. Luminescent Properties

The luminescence property of complex 1 in the solid state was investigated at room temperature. As shown in Figure 8, the maximal emission peak appears at 514 nm ($\lambda_{\text{ex}} = 415$ nm) and it displays a green color. In contrast, free DHTA has the maximum emission peak at 476 nm ($\lambda_{\text{ex}} = 325$ nm), with a blue-shift of 38 nm compared with complex 1. Moreover, the luminescence intensity of the complex 1 is 6000, which is much higher than DHTA of 5250. Moreover, the luminescence intensity of the complex is much higher than that of the ligand. Compared with the spectrum of DHTA, the spectrum of complex 1 has a similar emission band and location, indicating that the intra-ligand transition is responsible for the emission of complex 1 [31], the enhancement and the red-shift of the luminescence emissions in complex 1 may be attributed to the increased energy transfer efficiency between the ligand and metal ions after the formation of the complex, which reduces the energy loss and further enhances the rigidity of the molecule, resulting in a significant increase in luminescent intensity. These results suggest that complex 1 may have potential applications as a new green luminescence material.

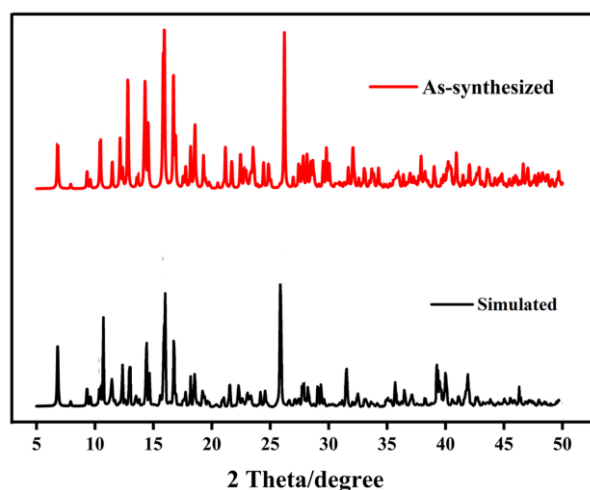


Figure 7. PXRD of complex 1.

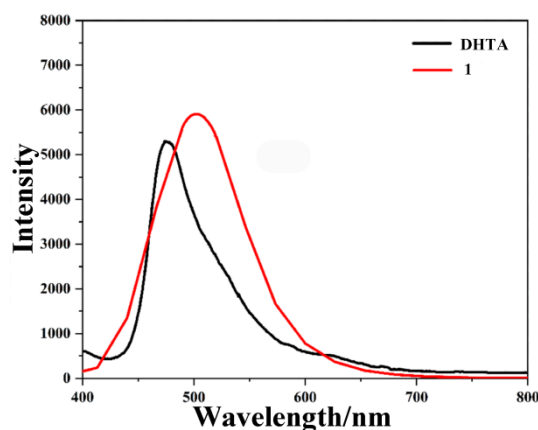


Figure 8. Solid-state emission spectrum of **1** and DHTA at room temperature.

4. Conclusions

In this work, we report a novel three-dimensional Ho(III) coordination polymer composed of DHTA and coordination water molecules. In the structure, one DHTA ligand acts as tridentate bridging ligand to connect the two Ho(III) through one hydroxyl oxygen atom and two carbonyl oxygen atoms, and the other six DHTA ligands coordinate with holmium atoms as bidentate ligands, and further form a stable 3D supramolecular network structure. IR spectrum indicates that the carboxyl group is coordinated to Ho(III) ion. The PXRD analysis showed that complex **1** was almost pure crystalline phase. According to TGA analysis, the complex **1** possesses a high thermal stability and good luminescence property. It also suggests that rare earth coordination polymers involving DHTA ligand and Ho(III) ions could contribute to the study of luminescence materials. These properties are expected to have further applications in the future.

Supplementary Materials: The following are available online at <https://www.mdpi.com/article/10.3390/cryst11111294/s1>, Table S1: Selected Bond Lengths (Å) and Bond Angles (°) of **1**, Table S2: Hydrogen Bond Length (Å) and Bond Angle (°) of **1**, Table S3: Short Ring-Interactions with Cg-Cg Distances < 4.0 Å, α < 20.000° and β < 60.0°. And the Analysis of C-H...Cg (π -Ring) Interactions (H...Cg < 3.0 Å, γ < 30.0°) for **1**.

Author Contributions: J.L. performed an experiment and wrote the article. L.D. conducted data processing and analysis. C.L. made structural characterization. F.Z. and Z.S. designed the experiments and conceived the project. All authors have read and agreed to the published version of the manuscript.

Funding: We appreciated the program of Jilin Provincial Department of Education (JJKH20200758KJ) for financial support.

Acknowledgments: The authors thank Changchun University of Science and Technology.

Conflicts of Interest: The authors declare no conflict of interest.

References

1. O’Keeffe, M.; Yaghi, O.M. Deconstructing the crystal structures of metal-organic frameworks and related materials into their underlying nets. *Chem. Rev.* **2012**, *112*, 675–702. [CrossRef] [PubMed]
2. Fan, W.D.; Zhang, X.R.; Kang, Z.X.; Liu, X.P.; Sun, D.F. Isoreticular chemistry within metal-organic frameworks for gas storage and separation. *Coord. Chem. Rev.* **2021**, *440*, 213968–214025. [CrossRef]
3. McCarver, G.A.; Rajeshkumar, T.; Vogiatzis, K.D. Computational catalysis for metal-organic frameworks: An overview. *Coord. Chem. Rev.* **2021**, *440*, 213777–213806. [CrossRef]
4. Zhu, X.D.; Zhang, K.; Wang, Y.; Long, W.W.; Sa, R.J.; Liu, T.F.; Lü, J. Fluorescent metal-organic framework (MOF) as a highly sensitive and quickly responsive chemical sensor for the detection of antibiotics in simulated wastewater. *Inorg. Chem.* **2018**, *57*, 1060–1065. [CrossRef]
5. Yang, X.L.; Chen, X.H.; Hou, G.H.; Guan, R.F.; Shao, R.; Xie, M.H. A multiresponsive metal-organic framework: Direct chemiluminescence, photoluminescence, and dual tunable sensing applications. *Adv. Funct. Mater.* **2016**, *26*, 393–398. [CrossRef]
6. Zhao, L.; Azhar, M.R.; Li, X.J.; Duan, X.G.; Sun, H.Q.; Wang, S.B.; Fang, X.C. Adsorption of cerium (III) by HKUST-1 metal-organic framework from aqueous solution. *J. Colloid Interface Sci.* **2019**, *542*, 421–428. [CrossRef]
7. Zhou, Y.; Yang, Q.; Zhang, D.N.; Gan, N.; Li, Q.P.; Cuan, J. Detection and removal of antibiotic tetracycline in water with a highly stable luminescent MOF. *J. Colloid Interface Sci.* **2018**, *262*, 137–143. [CrossRef]
8. Feng, X.; Shi, X.G.; Sun, Q.; Wang, L.Y.; Zhao, J.S.; Liu, Y.Y. Hydrothermal synthesis, crystal structure, and properties of A 3D holmium(III) coordination framework based on the pyridine 2,6-dicarboxylate and oxalate ligands, synth. *React. Inorg. Met.-Org. Nano-Met. Chem.* **2010**, *40*, 479–484.
9. Czaja, M.; Bodył-Gajowska, S.; Lisiecki, R.; Meijerink, A.; Mazurak, Z. The luminescence properties of rare-earth ions in natural fluorite. *Phys. Chem. Miner.* **2012**, *39*, 639–648. [CrossRef]
10. Fang, H.W.; Wei, X.T.; Zhou, S.S.; Li, X.Y.; Chen, Y.H.; Duan, C.K.; Yin, M. Terbium and holmium codoped yttrium phosphate as non-contact optical temperature sensors. *RSC Adv.* **2017**, *7*, 10200–10205. [CrossRef]
11. Zhou, J.M.; Shi, W.; Xu, N.; Cheng, P. Highly selective luminescent sensing of fluoride and organic small-molecule pollutants based on novel lanthanide metal-organic frameworks. *Inorg. Chem.* **2013**, *52*, 8082–8090. [CrossRef] [PubMed]
12. Wang, X.L.; Mu, B.; Lin, H.Y.; Yang, S.; Liu, G.C.; Tiana, A.X.; Zhang, J.W. Assembly and properties of transition-metal coordination polymers based on semi-rigid bis-pyridyl-bis-amide ligand: Effect of polycarboxylates on the dimensionality. *Dalton Trans.* **2012**, *41*, 11074–11084. [CrossRef]
13. Dong, X.Y.; Si, C.D.; Fan, Y.; Hu, D.C.; Yao, X.Q.; Yang, Y.X.; Liu, J.C. Effect of N-donor ligands and metal ions on the coordination polymers based on a semirigid carboxylic acid ligand: Structures analysis, magnetic properties, and photoluminescence. *Cryst. Growth Des.* **2016**, *16*, 2062–2073. [CrossRef]
14. Bing, Y.Y.; Yua, M.H.; Hu, M. Synthesis, structures, and properties of seven transition metal coordination polymers based on a long semirigid dicarboxylic acid ligand. *RSC Adv.* **2015**, *5*, 47216–47224. [CrossRef]
15. Wang, X.F.; Liu, G.X. Syntheses and crystal structures of three Cu(II) coordination polymers based on 1,3,5-tris(imidazol-1-yl)benzene and benzene carboxylate ligands. *J. Chem. Crystallogr.* **2016**, *46*, 252–261. [CrossRef]
16. Wen, Y.H.; Dou, R.T.; Yao, K.; Xu, G.F. Syntheses, structures, and fluorescent properties of four Co(II) coordination polymers based on 5-hydroxyisophthalic acid and structurally related bis(benzimidazole) ligands. *J. Coord. Chem.* **2015**, *68*, 38–54. [CrossRef]
17. Wang, Y.; He, M.H.; Tian, Z.; Zhong, H.Y.; Zhu, S.L.; Zhang, Y.Y.; Zhang, X.P.; Chen, D.L.; He, Y.B. Rational construction of an ssa-type of MOF through pre-organizing the ligand’s conformation and its exceptional gas adsorption properties. *Dalton Trans.* **2018**, *47*, 2444–2452. [CrossRef]
18. Qiu, S.L.; Zhu, G.S. Molecular engineering for synthesizing novel structures of metal-organic frameworks with multifunctional properties. *Coord. Chem. Rev.* **2009**, *253*, 2891–2911. [CrossRef]
19. Wang, Y.L.; Jiang, Y.L.; Liu, Q.Y.; Tan, Y.X.; Wei, J.J.; Zhang, J. A series of three-dimensional lanthanide(iii) coordination polymers of 2,5-dihydroxy-1,4-benzenedicarboxylic acid based on dinuclear lanthanide units. *Cryst. Eng. Comm.* **2011**, *13*, 4981–4987. [CrossRef]
20. Wolfe, J.F.; Arnold, F.E. Rigid-rod polymers synthesis and thermal properties of para-aromatic polymers with 2,6-benzobisoxazole units in the main chain. *Macromolecules* **1981**, *14*, 909–915. [CrossRef]
21. Zhang, T.; Hu, D.; Jin, J.; Yang, S.L.; Li, G.; Jiang, J.M. Improvement of surface wettability and interfacial adhesion ability of poly(p-phenylene benzobisoxazole)(PBO) fiber by incorporation of 2,5-dihydroxyterephthalic acid (DHTA). *Eur. Polym. J.* **2009**, *45*, 302–307. [CrossRef]
22. CrysAlisPro (Version 1. 171. 31. 7.), Agilent Technologies. Available online: https://www.agilent.com/cs/library/usermanuals/Public/CrysAlis_Pro_User_Manual.pdf (accessed on 20 October 2021).
23. Sheldrick, G.M. SHELXT-integrated space-group and crystal-structure determination. *Acta Cryst.* **2015**, *71*, 3–8. [CrossRef]

24. Dolomanov, O.V.; Bourhis, L.J.; Gildea, R.J.; Howard, J.A.K.; Puschmann, H. OLEX2: A complete structure solution, refinement and analysis program. *J. Appl. Crystallogr.* **2009**, *42*, 339–341. [[CrossRef](#)]
25. Gao, Z.Q.; Lv, D.Y.; Gu, J.Z.; Li, H.J. Poly [[triqua(1 3-4-oxidopyridine-2,6-dicarboxylato)holmium(III)] monohydrate]. *Acta Cryst.* **2011**, *67*, 740–751. [[CrossRef](#)] [[PubMed](#)]
26. Thomas, S. The hydrogen bond in the solid state. *Angew. Chem. Int.* **2002**, *41*, 48–76.
27. Filippini, G.; Gavezzotti, A. Empirical intermolecular potentials for organic crystals: The ‘6-exp’ approximation revisited. *Acta Crystallogr. Sect.* **1993**, *49*, 868–880. [[CrossRef](#)]
28. Pamela, J.H.; Douglas, H. Organic-inorganic hybrid materials: From “simple coordination polymers to organodiamine-templated molybdenum oxides. *Angew. Chem. Int. Ed.* **1999**, *38*, 2638–2684.
29. Seddon, K.R. Infrared and raman spectra of inorganic and coordination compounds. *J. Organomet. Chem.* **1987**, *326*, C92–C93. [[CrossRef](#)]
30. Ren, Y.X.; Chen, S.P.; Gao, S.L. Preparation, crystal structure and enthalpy change of formation of the reaction in liquid phase of a new three-dimensional mixed-ligand holmium(III) coordination polymer based on strong π - π stacking interactions. *Chin. J. Chem.* **2007**, *25*, 63–67. [[CrossRef](#)]
31. Liu, C.L.; Zhang, R.L.; Lin, C.S.; Zhou, L.P.; Cai, L.X.; Kong, J.T.; Yang, S.Q.; Han, K.L.; Sun, Q.F. Intra-ligand charge transfer sensitization on self-assembled europium tetrahedral cage leads to dual selective luminescent sensing toward anion and cation. *J. Am. Chem. Soc.* **2017**, *139*, 12474–12479. [[CrossRef](#)]